International Journal of Automation and Computing
www.ijac.net

18(6), December 2021, 1007-1016
DOI: 10.1007/s11633-020-1268-6

Observer-based Multirate Feedback Control Design for Two-time-scale System

Ravindra Munje[1] Wei-Dong Zhang[2]

[1] Department of Electrical Engineering, K. K. Wagh Institute of Engineering Education and Research, Nashik 422003, India

[2] Department of Automation, Shanghai Jiao Tong University, Shanghai 200240, China

Abstract: The use of a lower sampling rate for designing a discrete-time state feedback-based controller fails to capture information of fast states in a two-time-scale system, while the use of a higher sampling rate increases the amount of computation considerably. Thus, the use of single-rate sampling for systems with slow and fast states has evident limitations. In this paper, multirate state feedback (MRSF) control for a linear time-invariant two-time-scale system is proposed. Here, multirate sampling refers to the sampling of slow and fast states at different sampling rates. Firstly, a block-triangular form of the original continuous two-time-scale system is constructed. Then, it is discretized with a smaller sampling period and feedback control is designed for the fast subsystem. Later, the system is block-diagonalized and equivalently represented into a system with a higher sampling period. Subsequently, feedback control is designed for the slow subsystem and overall MRSF control is derived. It is proved that the derived MRSF control stabilizes the full-order system. Being the transformed states of the original system, slow and fast states need to be estimated for the MRSF control realization. Hence, a sequential two-stage observer is formulated to estimate these states. Finally, the applicability of the design method is demonstrated with a numerical example and simulation results are compared with the single-rate sampling method. It is found that the proposed MRSF control and observer designs reduce computations without compromising closed-loop performance.

Keywords: Feedback control, multirate sampling, sequential observer, two-stage design, two-time-scale system.

Citation: R. Munje, W. D. Zhang. Observer-based multirate feedback control design for two-time-scale system. *International Journal of Automation and Computing*, vol.18, no.6, pp.1007–1016, 2021. http://doi.org/10.1007/s11633-020-1268-6

1 Introduction

A fundamental problem in control engineering, i.e., designing a feedback controller for a linear system has gained much importance since an appropriately designed feedback control improves system stability and closed-loop performance. Owing to the recent advances in microelectronics and computing technology, feedback controls are invariably implemented digitally. Early developments in this area assumed uniform sampling rates for converting signals from analog to digital format and vice-versa. Later, it was realized that there is a need to include multirate sampling[1], due to an increase in computational load in large-scale digital control systems. Within the last few decades, several techniques have been proposed on the eigenvalue assignment of discrete-time systems using multirate sampling[2–4]. In [3], outputs are sampled at $1/T_s$ Hz by applying the inputs sampled at μ/T_s Hz, where μ is greater than or equal to the controllability index. Further, in [2], it is shown that the inputs in [3] can be sampled at a rate slower than μ/T_s Hz. While, in [4], the inputs are sampled at $1/T_s$ Hz and the outputs are sampled at ν/T_s Hz, where ν is the observability index. Very recently, an optimal controller is designed in [5] for a linear system using a multirate approach, in which states and inputs are sampled at different rates. However, in this method, all the states are sampled at the same sampling rate and it also requires an observer for implementation. Whereas, techniques in [2–4] provide sufficient freedom for eigenvalue assignment and obviate the need for the deployment of an observer by sampling inputs and outputs at different rates.

The techniques in [2–4] are also applied to the singularly perturbed systems[6–9], in which eigenvalues of the system are grouped as dominant (slow) eigenvalues and non-dominant (fast) eigenvalues[10]. As these techniques are based on the feedback of outputs, rather than states, they lack robustness. Further, in [7], the input changes from a large positive value to a large negative value several times at the early stage of transient response to regulate the state, making it less suitable for industrial applications. Also, in the case of systems with a smaller value for the singular perturbation parameter, they result in feedback gains with larger values due to ill-conditioned system matrices arising because of the eigenvalue group-

Research Article
Manuscript received April 16, 2020; accepted November 12, 2020; published online January 30, 2021
Recommended by Associate Editor James Whidborne
Colored figures are available in the online version at https://link.springer.com/journal/11633

ings. In such a situation, two-stage feedback control designs[11−13], employing single-rate sampling are found to be more useful. Nevertheless, it is worth noting that, the response of fast states is crucial during a short transient period. After that, the behavior of the system is mostly decided by the slow states. The use of a larger sampling period for feedback control design for such systems causes loss of information in fast varying states. On the other hand, a smaller sampling period increases online computations considerably. Hence, the design of feedback control at a single sampling rate is not advisable. Conversely, using a multirate sampling strategy, the designer can accommodate multiple sampling rates for the group of states, rather than a single sampling rate. Consequently, the closed-loop control performance can be enhanced.

The conceptual background for investigating multirate state feedback (MRSF) control for the systems with slow and fast varying modes is established in [14], in which two multirate sampling schemes have been suggested with their theoretical differences. In contrast to [2−4], where inputs and outputs are sampled at different rates, in [14] slow and fast varying states are sampled at different rates. Furthermore, Kando and Iwazwumt[15] recommended the design of optimal regulators via multirate sampling. Lennarston[16] demonstrated that the disturbances, not considered in [14, 15], can be efficiently handled by adding immeasurable states in the existing model, which are determined by an estimator. State estimation problems are further solved by reporting multi-stage continuous-time observers[17−19] and multirate observers[20−24]. In multirate observers, the two-time-scale system is considered with quasi-steady-state modeling which is accompanied by approximation. This approximation can be avoided by using similarity transformations for the exact separation of subsystems[17−19]. However, more algebraic equations need to be solved which increases computation time.

In this paper, multirate state feedback control is proposed for a two-time-scale system using block-diagonalization, in which slow and fast subsystem states are sampled at different rates. Firstly, the continuous-time system is transformed into an upper triangular form and then feedback controls are designed for two subsystems with different sampling periods. Then, a feedback control input with slow and fast states, sampled at different rates, is derived. Lastly, for control realization, slow and fast subsystem states are estimated by a sequential two-stage observer. The presented method reduces design complexity, computations, and signal processing time significantly and also improves system performance. The usefulness of the reported design is verified by simulating a numerical example.

The paper is organized as follows. In Section 2, the main results of this paper are presented. The application of the controller to the numerical example is illustrated in Section 3. Finally, the paper is concluded in Section 4.

2 Main results

2.1 System description

Consider a linear time-invariant continuous-time system

$$\dot{\boldsymbol{z}} = \boldsymbol{A}\boldsymbol{z} + \boldsymbol{B}\boldsymbol{u} \tag{1}$$

$$\boldsymbol{y} = \boldsymbol{C}\boldsymbol{z} \tag{2}$$

where $\boldsymbol{z} \in \mathbf{R}^n$, $\boldsymbol{u} \in \mathbf{R}^{\mathbf{m}}$ and $\boldsymbol{y} \in \mathbf{R}^p$ are states, inputs and outputs, respectively. If system (1)−(2) is assumed to have a two-time-scale structure, i.e., n eigenvalues have n_1 slow and n_2 fast eigenvalues, then it can be written as

$$\begin{bmatrix} \dot{\boldsymbol{z}}_1 \\ \dot{\boldsymbol{z}}_2 \end{bmatrix} = \begin{bmatrix} \boldsymbol{A}_{11} & \boldsymbol{A}_{12} \\ \dfrac{\boldsymbol{A}_{21}}{\varepsilon} & \dfrac{\boldsymbol{A}_{22}}{\varepsilon} \end{bmatrix} \begin{bmatrix} \boldsymbol{z}_1 \\ \boldsymbol{z}_2 \end{bmatrix} + \begin{bmatrix} \boldsymbol{B}_1 \\ \dfrac{\boldsymbol{B}_2}{\varepsilon} \end{bmatrix} \boldsymbol{u} \tag{3}$$

$$\boldsymbol{y} = \begin{bmatrix} \boldsymbol{C}_1 & \boldsymbol{C}_2 \end{bmatrix} \begin{bmatrix} \boldsymbol{z}_1^{\mathrm{T}} & \boldsymbol{z}_2^{\mathrm{T}} \end{bmatrix}^{\mathrm{T}} \tag{4}$$

where $\boldsymbol{z}_1 \in \mathbf{R}^{n_1}$ and $\boldsymbol{z}_2 \in \mathbf{R}^{n_2}$, such that $n_1 + n_2 = n$. Submatrices $\boldsymbol{A}_{ij}$, $\boldsymbol{B}_i$ and $\boldsymbol{C}_i$ are of compatible dimensions. Parameter ε is the speed ratio of the slow versus fast states.

Assumption 1. The pairs $(\boldsymbol{A}, \boldsymbol{B})$ and $(\boldsymbol{A}, \boldsymbol{C})$ are respectively controllable and observable[25].

Assumption 2. Matrix $\boldsymbol{A}_{22}$ is invertible[26].

Assumption 1 ensures state stabilization and estimation of (3)−(4) by the state feedback control and observer respectively. It also helps to fulfill the controllability and observability properties of the lower order continuous-time subsystems obtained in the next subsections by the application of similarity transformations. Assumption 2 is necessary to get solutions of algebraic equations deliberated on later in the design procedure.

As the states of the slow subsystem remain almost constant over a time duration of $1/\varepsilon$, it is reasonable to measure them at a slower sampling rate compared to the fast subsystem states. Therefore, if the fast states are sampled at the $\varDelta$ sampling interval, slow states can be sampled at τ sampling interval, where $\varDelta = \tau/N$ with N as the largest integer smaller or equal to $1/\varepsilon$ [16]. Interestingly, for a suitably selected value of a sampling interval, the discrete-time system equivalent to the continuous two-time-scale system (3)−(4), would also possess the two-time-scale property[17, 27]. Thus, the designer has to select N, τ and $\varDelta$. Out of these, N is selected, such that, it is $\leq 1/\varepsilon$. Now, if τ is selected, one can acquire $\varDelta$. Sampling period τ can be carefully chosen using sampling theorem[28] and Condition 1.

Condition 1. If Assumption 1 is satisfied and system (3) has only real eigenvalues, then any $T_s > 0$ can be taken, otherwise, if $|\mathrm{Re}(\lambda_i - \lambda_j)| = 0$, then

$$T_s \neq \frac{2\pi m}{|\Im m(\lambda_i - \lambda_j)|}, \quad \text{for } m = 1, 2, \cdots \tag{5}$$

where λ_i and λ_j are any two eigenvalues[25, 29].

Condition 1 is required to satisfy the controllability property of the discrete-time systems received by sampling the corresponding continuous-time system. It must be noted that, if τ meets the sampling theorem and Condition 1, $\varDelta$ also meets both.

Suppose the sampling begins at a $k\tau$ instant. Here, slow states are measured at every $k\tau$, where $k = 0, 1, 2, \cdots$, while the fast states are measured at every $\varDelta = k\tau/N$. In other words, in the τ sampling interval of slow states, fast states are sampled N times at every $l\varDelta$, where $l = 0, 1, 2, \cdots, (N-1)$. The overall feedback control input is the combination of slow and fast controls, such that

$$\boldsymbol{u}(t) = \boldsymbol{u}_s(k\tau) + \boldsymbol{u}_f(k\tau + l\varDelta) \tag{6}$$

where $\boldsymbol{u}_s(k\tau)$ and $\boldsymbol{u}_f(k\tau + l\varDelta)$ are piece-wise constant during $k\tau \leq t < (k+1)\tau$ and $k\tau + l\Delta \leq t < k\tau + (l+1)\Delta$, respectively.

Even if the singular perturbation parameter ε does not need to appear explicitly in the system, the system can still have slow and fast eigenvalues. Hence, the use of similarity transformation matrices to derive decoupled subsystems could be a more promising and accurate method instead of singular perturbation methods[30]. The proposed observed-based multirate feedback control design uses similarity transformations. In the following subsections, the complete design scheme of MRSF control and state estimation by the sequential observer are presented.

2.2 MRSF control design for two-time-scale system

First of all, an upper triangular form of (3) is constructed and then its discrete-time forms are acquired sequentially, starting from a lower to higher sampling periods, i.e., $\varDelta \to \tau$. Just after achieving a particular discrete-time form, feedback control for the corresponding uncoupled subsystem is designed. The block-triangular form of (3) is given by

$$\begin{bmatrix} \dot{\boldsymbol{z}}_1 \\ \dot{\boldsymbol{z}}_f \end{bmatrix} = \begin{bmatrix} \boldsymbol{A}_s & \boldsymbol{A}_{12} \\ \boldsymbol{0} & \dfrac{\boldsymbol{A}_f}{\varepsilon} \end{bmatrix} \begin{bmatrix} \boldsymbol{z}_1 \\ \boldsymbol{z}_f \end{bmatrix} + \begin{bmatrix} \boldsymbol{B}_1 \\ \dfrac{\boldsymbol{B}_f}{\varepsilon} \end{bmatrix} \boldsymbol{u}. \tag{7}$$

In (7), $\max|\mathrm{Re}\,\{\lambda(\boldsymbol{A}_s)\}| << \min\left|\mathrm{Re}\left\{\lambda\left(\dfrac{\boldsymbol{A}_f}{\varepsilon}\right)\right\}\right|$, where $\lambda(\cdot)$ is the eigenvalue. System in (7) is obtained by applying the state variable transformation given below:

$$\begin{bmatrix} \boldsymbol{z}_1 \\ \boldsymbol{z}_f \end{bmatrix} = \begin{bmatrix} \boldsymbol{I}_{n1} & \boldsymbol{0} \\ \boldsymbol{P} & \boldsymbol{I}_{n2} \end{bmatrix} \begin{bmatrix} \boldsymbol{z}_1 \\ \boldsymbol{z}_2 \end{bmatrix} \tag{8}$$

to the system in (3), in which $\boldsymbol{I}_n$ is an identity matrix of order n and matrix $\boldsymbol{P}$ satisfies

$$\varepsilon \boldsymbol{P}(\boldsymbol{A}_{11} - \boldsymbol{A}_{12}\boldsymbol{P}) + \boldsymbol{A}_{21} - \boldsymbol{A}_{22}\boldsymbol{P} = 0 \tag{9}$$

where $\boldsymbol{A}_s = \boldsymbol{A}_{11} - \boldsymbol{A}_{12}\boldsymbol{P}$, $\boldsymbol{A}_f = \varepsilon\boldsymbol{P}\boldsymbol{A}_{12} + \boldsymbol{A}_{22}$ and $\boldsymbol{B}_f = \varepsilon\boldsymbol{P}\boldsymbol{B}_1 + \boldsymbol{B}_2$. The solution of (9) exists for a sufficiently small value of ε and under Assumption 2. Setting $\varepsilon = 0$ in (9) gives $\boldsymbol{A}_{21} - \boldsymbol{A}_{22}\boldsymbol{P}^{(0)} = 0$, i.e., $\boldsymbol{P}^{(0)} = \boldsymbol{A}_{22}^{-1}\boldsymbol{A}_{21} \Longrightarrow \boldsymbol{P}^{(0)} = \boldsymbol{A}_{22}^{-1}\boldsymbol{A}_{21}$ and $\boldsymbol{P}^{(0)} = O(1)$ and $\boldsymbol{P} = \boldsymbol{P}^{(0)} + O(\varepsilon)$. Having found $\boldsymbol{P}^{(0)}$, the algebraic equation (9) can be solved by the fixed point iteration method[31]. Assumption 1 implies system (7) is controllable. In (7), the fast subsystem is entirely isolated from the slow subsystems. At this point, according to Assumption 1, controllability of $\left(\dfrac{\boldsymbol{A}_f}{\varepsilon}, \dfrac{\boldsymbol{B}_f}{\varepsilon}\right)$ is preserved. Now, the system (7) is discretized with the $\triangle$ sampling interval as

$$\begin{bmatrix} \boldsymbol{z}_{1,l+1} \\ \boldsymbol{z}_{f,l+1} \end{bmatrix} = \begin{bmatrix} \boldsymbol{\Phi}_{\varDelta s} & \boldsymbol{\Phi}_{\varDelta 12} \\ \boldsymbol{0} & \boldsymbol{\Phi}_{\varDelta f} \end{bmatrix} \begin{bmatrix} \boldsymbol{z}_{1,l} \\ \boldsymbol{z}_{f,l} \end{bmatrix} + \begin{bmatrix} \boldsymbol{\Gamma}_{\varDelta 1} \\ \boldsymbol{\Gamma}_{\varDelta f} \end{bmatrix} \boldsymbol{u}_l \tag{10}$$

where

$$\begin{bmatrix} \boldsymbol{\Phi}_{\varDelta s} & \boldsymbol{\Phi}_{\varDelta 12} \\ \boldsymbol{0} & \boldsymbol{\Phi}_{\varDelta f} \end{bmatrix} = \bar{\boldsymbol{\Phi}}_{\varDelta} = \mathrm{e}^{\bar{\boldsymbol{A}}\varDelta}$$

$$\begin{bmatrix} \boldsymbol{\Gamma}_{\varDelta 1} \\ \boldsymbol{\Gamma}_{\varDelta f} \end{bmatrix} = \bar{\boldsymbol{\Gamma}}_{\varDelta} = \int_0^{\varDelta} \mathrm{e}^{\bar{\boldsymbol{A}}\eta}\bar{\boldsymbol{B}}\mathrm{d}\eta$$

in which

$$\bar{\boldsymbol{A}} = \begin{bmatrix} \boldsymbol{A}_s & \boldsymbol{A}_{12} \\ \boldsymbol{0} & \dfrac{\boldsymbol{A}_f}{\varepsilon} \end{bmatrix}, \qquad \bar{\boldsymbol{B}} = \begin{bmatrix} \boldsymbol{B}_1 \\ \dfrac{\boldsymbol{B}_f}{\varepsilon} \end{bmatrix}.$$

Feedback control design for (10) requires the following Assumption 3.

Assumption 3. System $(\bar{\boldsymbol{\Phi}}_{\triangle}, \bar{\boldsymbol{\Gamma}}_{\triangle})$ is controllable.

If sampling periods (τ and $\triangle$) meet the sampling theorem[28] and Condition 1, Assumption 3 is fulfilled. As a result, the controllability of $(\bar{\boldsymbol{\Phi}}_{\triangle}, \bar{\boldsymbol{\Gamma}}_{\triangle})$ infers the controllability of $(\boldsymbol{\Phi}_{\varDelta f}, \boldsymbol{\Gamma}_{\varDelta f})$. And so, in the first stage, feedback control

$$\boldsymbol{u}_l = -\boldsymbol{F}_f\boldsymbol{z}_{f,l} + \boldsymbol{u}_{s,l} \tag{11}$$

is designed and applied to (10) as

$$\begin{bmatrix} \boldsymbol{z}_{1,l+1} \\ \boldsymbol{z}_{f,l+1} \end{bmatrix} = \begin{bmatrix} \boldsymbol{\Phi}_{\varDelta s} & \boldsymbol{\Phi}_{\varDelta 12} - \boldsymbol{\Gamma}_{\varDelta 1}\boldsymbol{F}_f \\ \boldsymbol{0} & \boldsymbol{\Phi}_{\varDelta f} - \boldsymbol{\Gamma}_{\varDelta f}\boldsymbol{F}_f \end{bmatrix} \begin{bmatrix} \boldsymbol{z}_{1,l} \\ \boldsymbol{z}_{f,l} \end{bmatrix} + \begin{bmatrix} \boldsymbol{\Gamma}_{\varDelta 1} \\ \boldsymbol{\Gamma}_{\varDelta f} \end{bmatrix} \boldsymbol{u}_{s,l}. \tag{12}$$

The feedback gain $\boldsymbol{F}_f$ is chosen, such that $\lambda(\boldsymbol{\Phi}_{\Delta f} - \boldsymbol{\Gamma}_{\Delta f}\boldsymbol{F}_f) = \lambda_{\Delta f}^{desired}$ and is positioned near the origin. After that, system (12) is modified to

$$\begin{bmatrix} \boldsymbol{z}_{s,l+1} \\ \boldsymbol{z}_{f,l+1} \end{bmatrix} = \begin{bmatrix} \boldsymbol{\Phi}_{\Delta s} & \boldsymbol{0} \\ \boldsymbol{0} & \boldsymbol{\Phi}_{\Delta f} - \boldsymbol{\Gamma}_{\Delta f}\boldsymbol{F}_f \end{bmatrix} \begin{bmatrix} \boldsymbol{z}_{s,l} \\ \boldsymbol{z}_{f,l} \end{bmatrix} + \begin{bmatrix} \boldsymbol{\Gamma}_{\Delta s} \\ \boldsymbol{\Gamma}_{\Delta f} \end{bmatrix} \boldsymbol{u}_{s,l} \tag{13}$$

to separate fast subsystems. This is achieved by applying

$$\begin{bmatrix} \boldsymbol{z}_{s,l} \\ \boldsymbol{z}_{f,l} \end{bmatrix} = \begin{bmatrix} \boldsymbol{I}_{n1} & -\boldsymbol{M} \\ \boldsymbol{0} & \boldsymbol{I}_{n2} \end{bmatrix} \begin{bmatrix} \boldsymbol{z}_{1,l} \\ \boldsymbol{z}_{f,l} \end{bmatrix} \tag{14}$$

to (12). In this, matrix $\boldsymbol{M}$ is evaluated by setting

$$\boldsymbol{\Phi}_{\Delta 12} - \boldsymbol{\Gamma}_{\Delta 1}\boldsymbol{F}_f + \boldsymbol{\Phi}_{\Delta s}\boldsymbol{M} - \boldsymbol{M}(\boldsymbol{\Phi}_{\Delta f} - \boldsymbol{\Gamma}_{\Delta f}\boldsymbol{F}_f) = 0. \tag{15}$$

Equation (15) can be solved using the "lyap" command of Matlab[32] as a linear algebraic Sylvester equation[25] with Assumption 4 given below.

Assumption 4. $\lambda(\boldsymbol{\Phi}_{\Delta s}) \neq \lambda(\boldsymbol{\Phi}_{\Delta f} - \boldsymbol{\Gamma}_{\Delta f}\boldsymbol{F}_f)$.

Assumption 4 is fulfilled because subsystem $(\boldsymbol{\Phi}_{\Delta f} - \boldsymbol{\Gamma}_{\Delta f}\boldsymbol{F}_f)$ is user designed with the eigenvalues close to the origin, whereas the subsystem $\boldsymbol{\Phi}_{\Delta s}$ has the original system's slow eigenvalues. Manipulating (12) and (14) gives $\boldsymbol{\Gamma}_{\Delta s} = \boldsymbol{\Gamma}_{\Delta 1} - \boldsymbol{M}\boldsymbol{\Gamma}_{\Delta f}$. System (13) has a sampling period of Δ seconds. If $\tau = N/\Delta$, the system corresponding to the τ sampling interval can be built from (13) as

$$\begin{bmatrix} \boldsymbol{z}_{s,k+1} \\ \boldsymbol{z}_{f,k+1} \end{bmatrix} = \begin{bmatrix} \boldsymbol{\Phi}_{\tau s} & \boldsymbol{0} \\ \boldsymbol{0} & \boldsymbol{\Phi}_{\tau f} \end{bmatrix} \begin{bmatrix} \boldsymbol{z}_{s,k} \\ \boldsymbol{z}_{f,k} \end{bmatrix} + \begin{bmatrix} \boldsymbol{\Gamma}_{\tau s} \\ \boldsymbol{\Gamma}_{\tau f} \end{bmatrix} \boldsymbol{u}_{s,k}. \tag{16}$$

The state and input matrices of the Δ system (13) and τ system (16) are related as $\boldsymbol{\Phi}_\tau = \boldsymbol{\Phi}_\Delta^N$ and $\boldsymbol{\Gamma}_\tau = \sum_{i=0}^{N-1} \boldsymbol{\Phi}_\Delta^i \boldsymbol{\Gamma}_\Delta$. As a result, submatrices in (16) are obtained as

$$\begin{cases} \boldsymbol{\Phi}_{\tau s} = \boldsymbol{\Phi}_{\Delta s}^N, \ \boldsymbol{\Gamma}_{\tau s} = \sum_{i=0}^{N-1} \boldsymbol{\Phi}_{\Delta s}^i \boldsymbol{\Gamma}_{\Delta s} \\ \boldsymbol{\Phi}_{\tau f} = (\boldsymbol{\Phi}_{\Delta f} - \boldsymbol{\Gamma}_{\Delta f}\boldsymbol{F}_f)^N, \\ \boldsymbol{\Gamma}_{\tau f} = \sum_{i=0}^{N-1} (\boldsymbol{\Phi}_{\Delta f} - \boldsymbol{\Gamma}_{\Delta f}\boldsymbol{F}_f)^i \boldsymbol{\Gamma}_{\Delta f}. \end{cases} \tag{17}$$

As the controllability of the slow subsystem $(\boldsymbol{\Phi}_{\tau s}, \boldsymbol{\Gamma}_{\tau s})$ is confirmed by Assumption 3, in the second stage,

$$\boldsymbol{u}_{s,k} = -\boldsymbol{F}_s \boldsymbol{z}_{s,k} \tag{18}$$

is designed and applied to (16) to have a closed-loop system

$$\begin{bmatrix} \boldsymbol{z}_{s,k+1} \\ \boldsymbol{z}_{f,k+1} \end{bmatrix} = \begin{bmatrix} \boldsymbol{\Phi}_{\tau s} - \boldsymbol{\Gamma}_{\tau s}\boldsymbol{F}_s & \boldsymbol{0} \\ -\boldsymbol{\Gamma}_{\tau f}\boldsymbol{F}_s & \boldsymbol{\Phi}_{\tau f} \end{bmatrix} \begin{bmatrix} \boldsymbol{z}_{s,k} \\ \boldsymbol{z}_{f,k} \end{bmatrix}. \tag{19}$$

In (19), the feedback gain $\boldsymbol{F}_s$ is selected, such that $\lambda(\boldsymbol{\Phi}_{\tau s} - \boldsymbol{\Gamma}_{\tau s}\boldsymbol{F}_s) = \lambda_{\tau s}^{desired}$ and are placed near the unit circle. Thus, the overall MRSF control is

$$\boldsymbol{u}(t) = -\boldsymbol{F}_f \boldsymbol{z}_{f,l} - \boldsymbol{F}_s \boldsymbol{z}_{s,k} \tag{20}$$

where

$$\boldsymbol{u}_{f,l} = -\boldsymbol{F}_f \boldsymbol{z}_{f,l}, \ k\tau + l\Delta \leq t < k\tau + (l+1)\Delta$$
$$\boldsymbol{u}_{s,k} = -\boldsymbol{F}_s \boldsymbol{z}_{s,k}, \ k\tau \leq t < (k+1)\tau.$$

Lemma 1. Input (20), received by sampling fast and slow subsystem states respectively at Δ and τ intervals, stabilizes system (19).

Proof. In a block-triangular system (19), eigenvalues are the disjoint sum of eigenvalues of diagonal matrices $\boldsymbol{\Phi}_{\tau s} - \boldsymbol{\Gamma}_{\tau s}\boldsymbol{F}_s$ and $\boldsymbol{\Phi}_{\tau f}$. The subsystem $(\boldsymbol{\Phi}_{\tau s} - \boldsymbol{\Gamma}_{\tau s}\boldsymbol{F}_s)$ is stabilized with $\boldsymbol{F}_s$, so that the eigenvalues stay within the unit circle near the perimeter. On the other hand, subsystem $\boldsymbol{\Phi}_{\tau f}$ is given by (17), in which the eigenvalues of $\boldsymbol{\Phi}_{\Delta f} - \boldsymbol{\Gamma}_{\Delta f}\boldsymbol{F}_f$ are stabilized by the feedback gain $\boldsymbol{F}_f$. At this instant, if $|\lambda(\boldsymbol{\Phi}_{\Delta f} - \boldsymbol{\Gamma}_{\Delta f}\boldsymbol{F}_f)| < 1$, then

$$|\lambda((\boldsymbol{\Phi}_{\Delta f} - \boldsymbol{\Gamma}_{\Delta f}\boldsymbol{F}_f)^N)| < 1 \tag{21}$$

making $|\lambda(\boldsymbol{\Phi}_{\tau f})| < 1$. As a deduction, input (20) stabilizes system (19). □

The control input (20) is obtained by designing feedback controls for the completely decoupled fast ($\boldsymbol{z}_f$) and slow ($\boldsymbol{z}_s$) subsystem states at different sampling rates. Being internal and decoupled states, they cannot be measured and sampled directly for implementing (20). For that reason, an observer is desired to estimate them separately, so that they can be sampled at different rates. As a result, control (20) becomes

$$\boldsymbol{u}(t) = -\boldsymbol{F}_f \hat{\boldsymbol{z}}_{f,l} - \boldsymbol{F}_s \hat{\boldsymbol{z}}_{s,k} \tag{22}$$

where $\hat{\boldsymbol{z}}_f$ and $\hat{\boldsymbol{z}}_s$ are estimates of the continuous-time fast and slow subsystem states respectively. These are then sampled with the Δ and τ sampling intervals to get the corresponding $\hat{\boldsymbol{z}}_{f,l}$ and $\hat{\boldsymbol{z}}_{s,k}$. In the next subsection, estimation of these states is discussed.

2.3 State estimation using sequential observer

The full-order observer for (3)−(4) can be constructed[25] as

$$\begin{bmatrix} \dot{\hat{\boldsymbol{z}}}_1 \\ \dot{\hat{\boldsymbol{z}}}_2 \end{bmatrix} = \begin{bmatrix} \boldsymbol{A}_{11} & \boldsymbol{A}_{12} \\ \frac{\boldsymbol{A}_{21}}{\varepsilon} & \frac{\boldsymbol{A}_{22}}{\varepsilon} \end{bmatrix} \begin{bmatrix} \hat{\boldsymbol{z}}_1 \\ \hat{\boldsymbol{z}}_2 \end{bmatrix} + \begin{bmatrix} \boldsymbol{B}_1 \\ \frac{\boldsymbol{B}_2}{\varepsilon} \end{bmatrix} \boldsymbol{u} + \begin{bmatrix} \boldsymbol{L}_1 \\ \frac{\boldsymbol{L}_2}{\varepsilon} \end{bmatrix} (\boldsymbol{y} - \hat{\boldsymbol{y}})$$
$$\dot{\hat{\boldsymbol{z}}} = \boldsymbol{A}\hat{\boldsymbol{z}} + \boldsymbol{B}\boldsymbol{u} + \boldsymbol{L}(\boldsymbol{y} - \hat{\boldsymbol{y}}) = (\boldsymbol{A} - \boldsymbol{L}\boldsymbol{C})\hat{\boldsymbol{z}} + \boldsymbol{B}\boldsymbol{u} + \boldsymbol{L}\boldsymbol{y} \tag{23}$$

$$\hat{\boldsymbol{y}} = \begin{bmatrix}\boldsymbol{C}_1 & \boldsymbol{C}_2\end{bmatrix}\begin{bmatrix}\hat{\boldsymbol{z}}_1^{\mathrm{T}} & \hat{\boldsymbol{z}}_2^{\mathrm{T}}\end{bmatrix}^{\mathrm{T}} = \boldsymbol{C}\hat{\boldsymbol{z}} \tag{24}$$

where $\hat{\boldsymbol{z}}_1$ and $\hat{\boldsymbol{z}}_2$ are estimates of $\boldsymbol{z}_1$ and $\boldsymbol{z}_2$, respectively. As transpose of the observer feedback matrix $\boldsymbol{A}^{\mathrm{T}}-\boldsymbol{C}^{\mathrm{T}}\boldsymbol{L}^{\mathrm{T}}$ generates the dual representation to the system feedback matrix $\boldsymbol{A}-\boldsymbol{B}\boldsymbol{K}$, a similar approach[17, 19] can be adapted to design $\boldsymbol{A}-\boldsymbol{B}\boldsymbol{K}$ and $\boldsymbol{A}-\boldsymbol{L}\boldsymbol{C}$. For this, consider a hypothetical system corresponding to (3)−(4) as

$$\begin{bmatrix}\dot{\boldsymbol{x}}_1\\ \dot{\boldsymbol{x}}_2\end{bmatrix} = \begin{bmatrix}\boldsymbol{A}_{11}^{\mathrm{T}} & \dfrac{\boldsymbol{A}_{21}^{\mathrm{T}}}{\varepsilon}\\ \boldsymbol{A}_{12}^{\mathrm{T}} & \dfrac{\boldsymbol{A}_{22}^{\mathrm{T}}}{\varepsilon}\end{bmatrix}\begin{bmatrix}\boldsymbol{x}_1\\ \boldsymbol{x}_2\end{bmatrix} + \begin{bmatrix}\boldsymbol{C}_1^{\mathrm{T}}\\ \boldsymbol{C}_2^{\mathrm{T}}\end{bmatrix}\upsilon \tag{25}$$

where $\boldsymbol{x}_1 \in \mathbf{R}^{n_1}$ and $\boldsymbol{x}_2 \in \mathbf{R}^{n_2}$. Introducing the state variable transformation:

$$\begin{bmatrix}\boldsymbol{q}_1\\ \boldsymbol{q}_2\end{bmatrix} = \begin{bmatrix}\boldsymbol{I}_{n1} & \boldsymbol{0}\\ \boldsymbol{0} & \dfrac{\boldsymbol{I}_{n2}}{\varepsilon}\end{bmatrix}\begin{bmatrix}\boldsymbol{x}_1\\ \boldsymbol{x}_2\end{bmatrix} = \boldsymbol{T}_1^{\mathrm{T}}\begin{bmatrix}\boldsymbol{x}_1\\ \boldsymbol{x}_2\end{bmatrix} \tag{26}$$

system (25) is changed to standard singular perturbation form:

$$\begin{bmatrix}\dot{\boldsymbol{q}}_1\\ \dot{\boldsymbol{q}}_2\end{bmatrix} = \begin{bmatrix}\boldsymbol{A}_{11}^{\mathrm{T}} & \boldsymbol{A}_{21}^{\mathrm{T}}\\ \dfrac{\boldsymbol{A}_{12}^{\mathrm{T}}}{\varepsilon} & \dfrac{\boldsymbol{A}_{22}^{\mathrm{T}}}{\varepsilon}\end{bmatrix}\begin{bmatrix}\boldsymbol{q}_1\\ \boldsymbol{q}_2\end{bmatrix} + \begin{bmatrix}\boldsymbol{C}_1^{\mathrm{T}}\\ \dfrac{\boldsymbol{C}_2^{\mathrm{T}}}{\varepsilon}\end{bmatrix}\upsilon. \tag{27}$$

Later, system (27) is structured to a lower triangular form:

$$\begin{bmatrix}\dot{\boldsymbol{q}}_s\\ \dot{\boldsymbol{q}}_2\end{bmatrix} = \begin{bmatrix}\boldsymbol{A}_s^{\mathrm{T}} & \boldsymbol{0}\\ \dfrac{\boldsymbol{A}_{12}^{\mathrm{T}}}{\varepsilon} & \dfrac{\boldsymbol{A}_f^{\mathrm{T}}}{\varepsilon}\end{bmatrix}\begin{bmatrix}\boldsymbol{q}_s\\ \boldsymbol{q}_2\end{bmatrix} + \begin{bmatrix}\boldsymbol{C}_s^{\mathrm{T}}\\ \dfrac{\boldsymbol{C}_2^{\mathrm{T}}}{\varepsilon}\end{bmatrix}\upsilon \tag{28}$$

by applying state transformation

$$\begin{bmatrix}\boldsymbol{q}_s\\ \boldsymbol{q}_2\end{bmatrix} = \begin{bmatrix}\boldsymbol{I}_{n1} & -\varepsilon\boldsymbol{P}^{\mathrm{T}}\\ \boldsymbol{0} & \boldsymbol{I}_{n2}\end{bmatrix}\begin{bmatrix}\boldsymbol{q}_1\\ \boldsymbol{q}_2\end{bmatrix} = \boldsymbol{T}_2^{\mathrm{T}}\begin{bmatrix}\boldsymbol{q}_1\\ \boldsymbol{q}_2\end{bmatrix} \tag{29}$$

to (27). Herein, the matrix $\boldsymbol{P}^{\mathrm{T}}$ is reckoned by solving

$$\varepsilon(\boldsymbol{A}_{11}^{\mathrm{T}} - \boldsymbol{P}^{\mathrm{T}}\boldsymbol{A}_{12}^{\mathrm{T}})\boldsymbol{P}^{\mathrm{T}} + \boldsymbol{A}_{21}^{\mathrm{T}} - \boldsymbol{P}^{\mathrm{T}}\boldsymbol{A}_{22}^{\mathrm{T}} = 0 \tag{30}$$

iteratively, in the same way as that of (9). After that, one can gain $\boldsymbol{A}_s^{\mathrm{T}} = \boldsymbol{A}_{11}^{\mathrm{T}} - \boldsymbol{P}^{\mathrm{T}}\boldsymbol{A}_{12}^{\mathrm{T}}$, $\boldsymbol{A}_f^{\mathrm{T}} = \varepsilon\boldsymbol{A}_{12}^{\mathrm{T}}\boldsymbol{P}^{\mathrm{T}} + \boldsymbol{A}_{22}$ and $\boldsymbol{C}_s^{\mathrm{T}} = \boldsymbol{C}_1^{\mathrm{T}} - \boldsymbol{P}^{\mathrm{T}}\boldsymbol{C}_2^{\mathrm{T}}$. Since $\lambda(\boldsymbol{A}) = \lambda(\boldsymbol{A}^{\mathrm{T}})$, system (28) also conforms to the eigenvalue grouping property of system (7). It is interesting to note that, the design of the feedback controller presented in Section 2.2 starts by decoupling the fast subsystem, as given by (12). Whereas the design of observer discussed in Section 2.2 is initiated by decoupling the slow subsystem, as shown by (28). This is due to the duality property, i.e., in designing the observer, the eigenvalue-assignment problem is solved for the dual system. For two-stage observer design, in the first stage, applying

$$\upsilon = -\boldsymbol{L}_s^{\mathrm{T}}\boldsymbol{q}_s + \upsilon_f \tag{31}$$

to system (28) leads to

$$\begin{bmatrix}\dot{\boldsymbol{q}}_s\\ \dot{\boldsymbol{q}}_2\end{bmatrix} = \begin{bmatrix}\boldsymbol{A}_s^{\mathrm{T}} - \boldsymbol{C}_s^{\mathrm{T}}\boldsymbol{L}_s^{\mathrm{T}} & \boldsymbol{0}\\ \dfrac{\boldsymbol{A}_{12}^{\mathrm{T}} - \boldsymbol{C}_2^{\mathrm{T}}\boldsymbol{L}_s^{\mathrm{T}}}{\varepsilon} & \dfrac{\boldsymbol{A}_f^{\mathrm{T}}}{\varepsilon}\end{bmatrix}\begin{bmatrix}\boldsymbol{q}_s\\ \boldsymbol{q}_2\end{bmatrix} + \begin{bmatrix}\boldsymbol{C}_s^{\mathrm{T}}\\ \dfrac{\boldsymbol{C}_2^{\mathrm{T}}}{\varepsilon}\end{bmatrix}\upsilon_f. \tag{32}$$

The slow subsystem observer gain $\boldsymbol{L}_s^{\mathrm{T}}$ is selected, such that $\lambda(\boldsymbol{A}_s^{\mathrm{T}} - \boldsymbol{C}_s^{\mathrm{T}}\boldsymbol{L}_s^{\mathrm{T}}) = \lambda_s^{desired}$. As the transformations (26) and (29) transmute the original system from (25) to (28) without losing controllability (or observability), the pair $(\boldsymbol{A}_s^{\mathrm{T}}, \boldsymbol{C}_s^{\mathrm{T}})$ is controllable (or the pair $(\boldsymbol{A}_s, \boldsymbol{C}_s)$ is observable), due to which an arbitrary eigenvalue assignment is possible under Assumption 1 for slow subsystem. Next, system (32) is restructured as

$$\begin{bmatrix}\dot{\boldsymbol{q}}_s\\ \dot{\boldsymbol{q}}_f\end{bmatrix} = \begin{bmatrix}\mathbf{A}_s^{\mathrm{T}} - \boldsymbol{C}_s^{\mathrm{T}}\boldsymbol{L}_s^{\mathrm{T}} & \boldsymbol{0}\\ \boldsymbol{0} & \dfrac{\boldsymbol{A}_f^{\mathrm{T}}}{\varepsilon}\end{bmatrix}\begin{bmatrix}\boldsymbol{q}_s\\ \boldsymbol{q}_f\end{bmatrix} + \begin{bmatrix}\boldsymbol{C}_s^{\mathrm{T}}\\ \dfrac{\boldsymbol{C}_f^{\mathrm{T}}}{\varepsilon}\end{bmatrix}\upsilon_f \tag{33}$$

by applying state variable transformation

$$\begin{bmatrix}\boldsymbol{q}_s\\ \boldsymbol{q}_f\end{bmatrix} = \begin{bmatrix}\boldsymbol{I}_{n1} & \boldsymbol{0}\\ \boldsymbol{H}^{\mathrm{T}} & \boldsymbol{I}_{n2}\end{bmatrix}\begin{bmatrix}\boldsymbol{q}_s\\ \boldsymbol{q}_2\end{bmatrix} = \boldsymbol{T}_3^{\mathrm{T}}\begin{bmatrix}\boldsymbol{q}_s\\ \boldsymbol{q}_2\end{bmatrix} \tag{34}$$

to system (32), in which $\boldsymbol{C}_f^{\mathrm{T}} = \boldsymbol{C}_2^{\mathrm{T}} + \varepsilon\boldsymbol{H}^{\mathrm{T}}\boldsymbol{C}_s^{\mathrm{T}}$ and

$$\varepsilon\boldsymbol{H}^{\mathrm{T}}(\boldsymbol{A}_s^{\mathrm{T}} - \boldsymbol{C}_s^{\mathrm{T}}\boldsymbol{L}_s^{\mathrm{T}}) + \boldsymbol{A}_{12}^{\mathrm{T}} - \boldsymbol{C}_2^{\mathrm{T}}\boldsymbol{L}_s^{\mathrm{T}} - \boldsymbol{A}_f^{\mathrm{T}}\boldsymbol{H}^{\mathrm{T}} = 0. \tag{35}$$

Just like (15), (35) can be solved to get $\boldsymbol{H}^{\mathrm{T}}$ with Assumption 5 given below.

Assumption 5. $\lambda(\boldsymbol{A}_s^{\mathrm{T}} - \boldsymbol{C}_s^{\mathrm{T}}\boldsymbol{L}_s^{\mathrm{T}}) \neq \lambda\left(\dfrac{\boldsymbol{A}_f^{\mathrm{T}}}{\varepsilon}\right)$.

Subsystem $(\boldsymbol{A}_s^{\mathrm{T}} - \boldsymbol{C}_s^{\mathrm{T}}\boldsymbol{L}_s^{\mathrm{T}})$ is user designed with asymptotically stable dominant eigenvalues and $\left(\dfrac{\boldsymbol{A}_f^{\mathrm{T}}}{\varepsilon}\right)$ has the original system's non-dominant eigenvalues. That being so, Assumption 5 is satisfied. Thereupon, in the second stage, passing input

$$\upsilon_f = -\boldsymbol{L}_f^{\mathrm{T}}\boldsymbol{q}_f \tag{36}$$

to the system (33) provides

$$\begin{bmatrix}\dot{\boldsymbol{q}}_s\\ \dot{\boldsymbol{q}}_f\end{bmatrix} = \begin{bmatrix}\boldsymbol{A}_s^{\mathrm{T}} - \boldsymbol{C}_s^{\mathrm{T}}\mathbf{L}_s^{\mathrm{T}} & -\boldsymbol{C}_s^{\mathrm{T}}\boldsymbol{L}_f^{\mathrm{T}}\\ \boldsymbol{0} & \dfrac{\boldsymbol{A}_f^{\mathrm{T}} - \boldsymbol{C}_f^{\mathrm{T}}\boldsymbol{L}_f^{\mathrm{T}}}{\varepsilon}\end{bmatrix}\begin{bmatrix}\boldsymbol{q}_s\\ \boldsymbol{q}_f\end{bmatrix}. \tag{37}$$

The fast subsystem observer gain $\boldsymbol{L}_f^{\mathrm{T}}$ is designed so as to place $\lambda(\boldsymbol{A}_f^{\mathrm{T}} - \boldsymbol{C}_f^{\mathrm{T}}\boldsymbol{L}_f^{\mathrm{T}})/\varepsilon = \lambda_f^{desired}$. Controllability of the fast subsystem $\left((\boldsymbol{A}_f^{\mathrm{T}})/\varepsilon, (\boldsymbol{C}_f^{\mathrm{T}})/\varepsilon\right)$ is preserved due to Assumption 1. Using inputs (31), (36) and transformations (26), (29) and (34), the overall observer gain is obtained as

$$\upsilon = \boldsymbol{L}^{\mathrm{T}}\boldsymbol{x} = \begin{bmatrix}\boldsymbol{L}_1^{\mathrm{T}} & \frac{1}{\varepsilon}\boldsymbol{L}_2^{\mathrm{T}}\end{bmatrix}\begin{bmatrix}\boldsymbol{x}_1^{\mathrm{T}} & \boldsymbol{x}_2^{\mathrm{T}}\end{bmatrix}^{\mathrm{T}} \tag{38}$$

where $\boldsymbol{L}_1^{\mathrm{T}} = -\boldsymbol{L}_s^{\mathrm{T}} - \boldsymbol{L}_f^{\mathrm{T}}\boldsymbol{H}^{\mathrm{T}}$ and $\boldsymbol{L}_2^{\mathrm{T}} = \varepsilon\boldsymbol{L}_s^{\mathrm{T}}\boldsymbol{P}^{\mathrm{T}} + \varepsilon\boldsymbol{L}_f^{\mathrm{T}}\boldsymbol{H}^{\mathrm{T}}\boldsymbol{P}^{\mathrm{T}} - \boldsymbol{L}_f^{\mathrm{T}}$. Once again, applying change of states

$$\begin{bmatrix}\boldsymbol{x}_s^{\mathrm{T}} & \boldsymbol{x}_f^{\mathrm{T}}\end{bmatrix}^{\mathrm{T}} = \boldsymbol{T}_1^{-\mathrm{T}}\begin{bmatrix}\boldsymbol{q}_s^{\mathrm{T}} & \boldsymbol{q}_f^{\mathrm{T}}\end{bmatrix}^{\mathrm{T}} \tag{39}$$

to the system (37) results in

$$\begin{bmatrix}\dot{\boldsymbol{x}}_s\\ \dot{\boldsymbol{x}}_f\end{bmatrix} = \begin{bmatrix}(\boldsymbol{A}_s - \boldsymbol{L}_s\boldsymbol{C}_s)^{\mathrm{T}} & \dfrac{-(\boldsymbol{L}_f\boldsymbol{C}_s)^{\mathrm{T}}}{\varepsilon}\\ \boldsymbol{0} & \dfrac{(\boldsymbol{A}_f - \boldsymbol{L}_f\boldsymbol{C}_f)^{\mathrm{T}}}{\varepsilon}\end{bmatrix}\begin{bmatrix}\boldsymbol{x}_s\\ \boldsymbol{x}_f\end{bmatrix}. \tag{40}$$

The hypothetical system (25) and system (40) are related by linear transformations (26), (29), (34) and (39) as

$$\begin{bmatrix}\boldsymbol{x}_s\\ \boldsymbol{x}_f\end{bmatrix} = \boldsymbol{T}^{\mathrm{T}}\begin{bmatrix}\boldsymbol{x}_1\\ \boldsymbol{x}_2\end{bmatrix} \Longrightarrow \begin{bmatrix}\boldsymbol{x}_1\\ \boldsymbol{x}_2\end{bmatrix} = \boldsymbol{T}^{-\mathrm{T}}\begin{bmatrix}\boldsymbol{x}_s\\ \boldsymbol{x}_f\end{bmatrix} \tag{41}$$

where

$$\boldsymbol{T}^{\mathrm{T}} = \boldsymbol{T}_1^{-\mathrm{T}}\boldsymbol{T}_3^{\mathrm{T}}\boldsymbol{T}_2^{\mathrm{T}}\boldsymbol{T}_1^{\mathrm{T}} = \begin{bmatrix}\boldsymbol{I}_{n_1} & -\boldsymbol{P}^{\mathrm{T}}\\ \varepsilon\boldsymbol{H}^{\mathrm{T}} & -\varepsilon\boldsymbol{H}^{\mathrm{T}}\boldsymbol{P}^{\mathrm{T}} + \boldsymbol{I}_{n_2}\end{bmatrix}. \tag{42}$$

Using (40) and the duality principle[19, 25], the observer can be configured as

$$\begin{bmatrix}\dot{\hat{\boldsymbol{z}}}_s\\ \dot{\hat{\boldsymbol{z}}}_f\end{bmatrix} = \begin{bmatrix}(\boldsymbol{A}_s - \boldsymbol{L}_s\boldsymbol{C}_s) & \boldsymbol{0}\\ \dfrac{-(\boldsymbol{L}_f\boldsymbol{C}_s)}{\varepsilon} & \dfrac{(\boldsymbol{A}_f - \boldsymbol{L}_f\boldsymbol{C}_f)}{\varepsilon}\end{bmatrix}\begin{bmatrix}\hat{\boldsymbol{z}}_s\\ \hat{\boldsymbol{z}}_f\end{bmatrix} + \begin{bmatrix}\boldsymbol{B}_{os}\\ \dfrac{\boldsymbol{B}_{of}}{\varepsilon}\end{bmatrix}\boldsymbol{u} + \begin{bmatrix}\boldsymbol{L}_s\\ \dfrac{\boldsymbol{L}_f}{\varepsilon}\end{bmatrix}\boldsymbol{y}. \tag{43}$$

The intriguing aspect is that the observer configuration (43) is matched with system (19) for state estimation. This is attainable only when feedback control and observer designs start with decoupling fast and slow subsystems respectively. Employing (41) for a two-time-scale system (23)−(24) gives

$$\begin{bmatrix}\hat{\boldsymbol{z}}_1^{\mathrm{T}} & \hat{\boldsymbol{z}}_2^{\mathrm{T}}\end{bmatrix}^{\mathrm{T}} = \boldsymbol{T}\begin{bmatrix}\hat{\boldsymbol{z}}_s^{\mathrm{T}} & \hat{\boldsymbol{z}}_f^{\mathrm{T}}\end{bmatrix}^{\mathrm{T}} \tag{44}$$

resulting in an observer that estimates slow and fast subsystem states as

$$\begin{bmatrix}\dot{\hat{\boldsymbol{z}}}_s\\ \dot{\hat{\boldsymbol{z}}}_f\end{bmatrix} = \boldsymbol{T}^{-1}(\boldsymbol{A} - \boldsymbol{L}\boldsymbol{C})\boldsymbol{T}\begin{bmatrix}\hat{\boldsymbol{z}}_s\\ \hat{\boldsymbol{z}}_f\end{bmatrix} + \boldsymbol{T}^{-1}\boldsymbol{B}\boldsymbol{u} + \boldsymbol{T}^{-1}\boldsymbol{L}\boldsymbol{y}. \tag{45}$$

Systems (43) and (45) are equivalent, in which case

$$\boldsymbol{T}^{-1}\boldsymbol{L} = \begin{bmatrix}\boldsymbol{L}_s\\ \dfrac{\boldsymbol{L}_f}{\varepsilon}\end{bmatrix} \Longrightarrow \boldsymbol{L} = \boldsymbol{T}\begin{bmatrix}\boldsymbol{L}_s\\ \dfrac{\boldsymbol{L}_f}{\varepsilon}\end{bmatrix}$$

can be verified using (38) and (42). Similarly, using $\boldsymbol{T}^{-1}\boldsymbol{B}$, one can get

$$\boldsymbol{B}_{os} = \boldsymbol{B}_1 - \varepsilon\boldsymbol{H}\boldsymbol{P}\boldsymbol{B}_1 - \boldsymbol{H}\boldsymbol{B}_2 \tag{46}$$

$$\boldsymbol{B}_{of} = \varepsilon\boldsymbol{P}\boldsymbol{B}_1 + \boldsymbol{B}_2. \tag{47}$$

In observer (43), the slow and fast states are estimated sequentially, in which case slow states are independent of the fast states and are used to estimate fast states. State estimation and its use in implementation of feedback control is illustrated in Fig. 1.

Novelty and benefits of the proposed sequential observer-based MRSF control design are listed below.

1) The MRSF control design is completed using two state variable transformations, compared to three state variable transformations in [11]. Also, in contrast to four state variable transformations in [19], only three state variable transformations are required to complete the two-stage design of sequential observer. As a result, manual design complexity is reduced significantly.

2) The offered design requires solutions of two algebraic equations for both MRSF control design and sequential observer design, i.e., solutions of four algebraic equations in all. Perversely, using straightforward designs in [11] and [19], solutions of six algebraic equations are required. As a lower number of algebraic equations need to be solved, the online computations are minimized.

3) The presented control design method uses the multirate sampling concept, due to which the online computations are reduced compared to the fast single-rate sampling[12], and the closed-loop performance is greatly improved compared to slower single-rate sampling[13].

4) In MRSF control, the on-line computations are reduced by around $n_1(N-1)$ in one τ sampling interval, compared to single-rate sampling control when designed with Δ seconds.

5) Since both designs (MRSF control and sequential observer) are done in two independent stages by the application of similarity transformations, eventual inaccuracies made in the second stage will not affect the first stage design accuracy.

The step-by-step design procedure is given below.

Step 1. Solve the algebraic (9) to get $\boldsymbol{P}$.

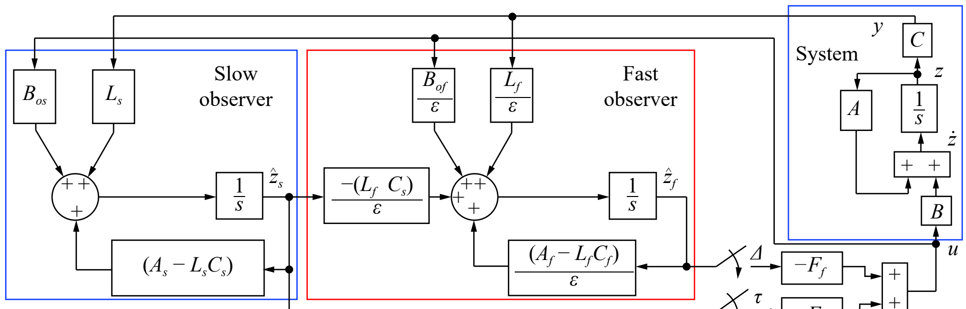

Fig. 1 Block diagram of observer-based controller design

Step 2. Determine $\boldsymbol{A}_s$, $\boldsymbol{A}_f$, $\boldsymbol{B}_f$ and construct system (7).

Step 3. Discretize (7) with Δ interval to get (10).

Step 4. Obtain $\boldsymbol{F}_f$, so that $\lambda(\boldsymbol{\Phi}_{\Delta f} - \boldsymbol{\Gamma}_{\Delta f}\boldsymbol{F}_f) = \lambda_{\Delta f}^{desired}$.

Step 5. Compute $\boldsymbol{M}$ by solving (15) and determine $\boldsymbol{\Gamma}_{\Delta s}$.

Step 6. Build (16) with τ interval using (17).

Step 7. Find out $\boldsymbol{F}_s$, so that $\lambda(\boldsymbol{\Phi}_{\tau s} - \boldsymbol{\Gamma}_{\tau s}\boldsymbol{F}_s) = \lambda_{\tau s}^{desired}$.

Step 8. Sample $\boldsymbol{z}_s$ and $\boldsymbol{z}_f$, obtained in Step 14, with τ and Δ intervals respectively and construct (20).

Step 9. Evaluate the algebraic equation (30) for $\boldsymbol{P}^{\mathrm{T}}$.

Step 10. Calculate $\boldsymbol{A}_s^{\mathrm{T}}$, $\boldsymbol{A}_f^{\mathrm{T}}$, $\boldsymbol{C}_s^{\mathrm{T}}$ and achieve system (28).

Step 11. Find out $\boldsymbol{L}_s^{\mathrm{T}}$, so that $\lambda(\boldsymbol{A}_s^{\mathrm{T}} - \boldsymbol{C}_s^{\mathrm{T}}\boldsymbol{L}_s^{\mathrm{T}}) = \lambda_s^{desired}$.

Step 12. Estimate $\boldsymbol{H}^{\mathrm{T}}$ by exercising (35) and get $\boldsymbol{C}_f^{\mathrm{T}}$.

Step 13. Obtain $\boldsymbol{L}_f^{\mathrm{T}}$, with $\lambda((\boldsymbol{A}_f^{\mathrm{T}} - \boldsymbol{C}_f^{\mathrm{T}}\boldsymbol{L}_f^{\mathrm{T}})/\varepsilon) = \lambda_f^{desired}$.

Step 14. Determine $\boldsymbol{B}_{os}$ and $\boldsymbol{B}_{of}$ in (46), (47) and formulate (43) for estimating $\boldsymbol{z}_s$ and $\boldsymbol{z}_f$.

3 Numerical example

Let us consider a fifth order steam power system[12], having two slow and three fast eigenvalues with the state, input and output matrices as

$$\boldsymbol{A} = \begin{bmatrix} -0.112\,5 & 0.046\,8 & 0.104\,9 & 0.000\,1 & 0.187\,6 \\ -0.000\,1 & -0.166\,9 & -0.000\,0 & -0.000\,2 & 0.626\,4 \\ -0.000\,0 & 1.333\,3 & -2.000\,1 & -0.000\,0 & -0.000\,4 \\ -2.000\,0 & 0.000\,1 & -0.000\,1 & -2.000\,1 & 0.000\,1 \\ 0.000\,6 & -0.000\,1 & 0.000\,7 & 1.267\,7 & -5.001\,4 \end{bmatrix}$$

$$\boldsymbol{B} = \begin{bmatrix} 0.000\,1 \\ 0.149\,9 \\ 0.000\,3 \\ 1.500\,3 \\ -0.002\,2 \end{bmatrix}, \quad \boldsymbol{C} = \begin{bmatrix} 1 & 1 & 0 & 0 & 0 \\ 0 & 0 & 1 & 1 & 1 \end{bmatrix}.$$

Eigenvalues are located at $(-5.033\,2,\ -1.969\,7 \pm 0.142\,8\mathrm{i},\ -0.154\,2 \pm 0.149\,4\mathrm{i})$ with the ratio of slow versus fast states as $\varepsilon = \dfrac{\max|\lambda_s|}{\min|\lambda_f|} = 0.108\,7$. Thus, N is taken as $9 \left(< \dfrac{1}{\varepsilon}\right)$. If the sampling duration for the slow subsystem is selected as $\tau = 1.8\,\mathrm{s}$, then the fast subsystem states are sampled at every $\Delta = 0.2\,\mathrm{s}$. Suppose the desired eigenvalues of the continuous-time system are $(-0.20, -0.35, -3.10, -4.30, -5.50)$. Consequently, the desired eigenvalues in z-domain for the slow and fast subsystems for τ and Δ sampling intervals respectively, can be obtained by $\mathrm{e}^{\lambda_i T_s}$, where λ_i is the i-th eigenvalue of the continuous-time system and T_s is the sampling period. Accordingly, $\lambda_{\Delta f}^{desired} = (0.537\,9, 0.423\,2, 0.332\,9)$ and $\lambda_{\tau s}^{desired} = (0.697\,7, 0.532\,6)$. Now, solution of (9) is found by the fixed point iteration method[31] to get $\boldsymbol{P}$ and an upper triangular form (7) is reached with

$$\boldsymbol{A}_s = \begin{bmatrix} -0.158\,2 & 0.126\,9 \\ -0.176\,1 & -0.150\,2 \end{bmatrix}, \quad \boldsymbol{B}_f = \begin{bmatrix} -0.011\,6 \\ 0.161\,9 \\ -0.000\,7 \end{bmatrix}$$

$$\boldsymbol{A}_f = \begin{bmatrix} -0.218\,3 & 0.000\,0 & -0.050\,2 \\ 0.012\,3 & -0.217\,5 & 0.017\,0 \\ 0.003\,3 & 0.137\,8 & -0.539\,9 \end{bmatrix}.$$

This system is then discretized with a sampling period of 0.2 s. Later, to place $\lambda_{\Delta f}^{desired}$, the feedback gain is determined as $\boldsymbol{F}_f = \begin{bmatrix} -5.727\,7 & 1.195\,9 & 0.898\,6 \end{bmatrix}$. Next, $\boldsymbol{M}$ is estimated to get (13) and subsequently system (16) with τ sampling interval is derived using (17), in which case

$$\boldsymbol{\Phi}_{\tau s} = \begin{bmatrix} 0.725\,0 & 0.171\,0 \\ -0.237\,3 & 0.735\,8 \end{bmatrix}, \quad \boldsymbol{\Gamma}_{\tau s} = \begin{bmatrix} 0.045\,8 \\ 0.540\,1 \end{bmatrix}$$

$$\boldsymbol{\Phi}_{\tau f} = \begin{bmatrix} 0.007\,1 & 0.000\,0 & -0.001\,1 \\ 0.034\,8 & 0.000\,2 & -0.005\,4 \\ 0.020\,5 & 0.000\,4 & -0.003\,0 \end{bmatrix}, \quad \boldsymbol{\Gamma}_{\tau f} = \begin{bmatrix} -0.036\,6 \\ 0.288\,4 \\ 0.073\,4 \end{bmatrix}.$$

The slow subsystem eigenvalues are placed at $\lambda_{\tau s}^{desired}$ by computing $\boldsymbol{F}_s = [-0.330\,7\ \ 0.454\,8]$. Utilizing obtained feedback gains, control input (20) is formulated. The system initial conditions are taken as (−0.2, 0.1, 0.1, −0.2, 0.4). States $\boldsymbol{z}_s$ and $\boldsymbol{z}_f$ are estimated using the sequential observer and are sampled at τ and Δ sampling intervals respectively, with desired observer eigenvalues as (−1.6, −1.8, −9.8, −11.2, −13.1). For this, the solution of (30) is determined and system (28) is obtained. $\boldsymbol{P}^{\mathrm{T}}$ in (30) and $\boldsymbol{A}_s^{\mathrm{T}}$ and $\boldsymbol{A}_f^{\mathrm{T}}$ in (28) are the exact transpose matrices of $\boldsymbol{P}$ in (9) and $\boldsymbol{A}_s$ and $\boldsymbol{A}_f$ in (7) respectively. After that, $\boldsymbol{C}_s^{\mathrm{T}}$ in (28) is obtained and then, to position $\lambda_s^{desired}$, the observer gain $\boldsymbol{L}_s^{\mathrm{T}}$ is determined. These are given below:

$$\boldsymbol{C}_s^{\mathrm{T}} = \begin{bmatrix} 1.000\,0 & -1.291\,5 \\ 1.000\,0 & 0.816\,8 \end{bmatrix}, \ \boldsymbol{L}_s^{\mathrm{T}} = \begin{bmatrix} 0.636\,3 & 0.942\,4 \\ -0.623\,6 & 0.866\,0 \end{bmatrix}.$$

Then, $\boldsymbol{H}^{\mathrm{T}}$ is calculated to gain (33) with

$$\boldsymbol{C}_f^{\mathrm{T}} = \begin{bmatrix} 2.337\,5 & 7.611\,7 \\ -0.729\,3 & 3.751\,6 \\ -0.557\,0 & 0.563\,4 \end{bmatrix}.$$

The fast subsystem eigenvalues are placed at $\lambda_f^{desired}$ by determining

$$\boldsymbol{L}_f^{\mathrm{T}} = \begin{bmatrix} 0.427\,4 & -1.471\,0 & 1.477\,5 \\ -0.004\,3 & 0.478\,5 & -0.494\,7 \end{bmatrix}.$$

Finally, $\boldsymbol{B}_{os}$ and $\boldsymbol{B}_{of}$ are calculated using (46) and (47), respectively as

$$\boldsymbol{B}_{os} = \begin{bmatrix} 2.125\,7 \\ -0.642\,8 \end{bmatrix}, \ \boldsymbol{B}_{of} = \begin{bmatrix} -0.011\,6 \\ 0.161\,9 \\ -0.000\,7 \end{bmatrix}.$$

Initial conditions for the estimated states of the original system (23) are obtained as given in [19] and initial conditions for the decoupled states are obtained from the relation (44). Using all these feedback and observer gains, initial conditions and other submatrices, the overall system is simulated. The simulation results are compared with the single-rate sampling videlicet Δ and τ seconds. Figs. 2 and 3 depict estimation errors of the decoupled and sampled slow and fast subsystem states, respectively.

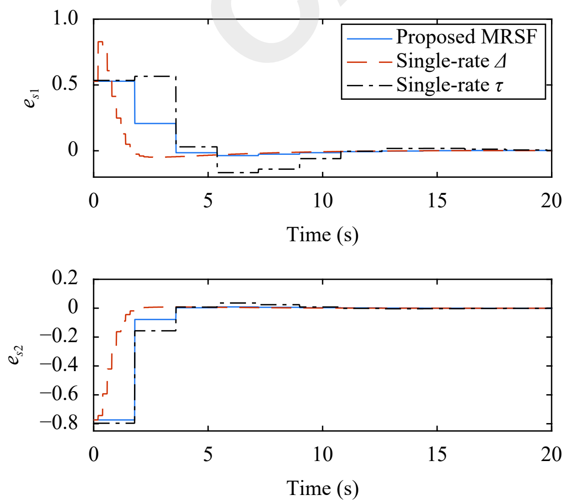

Fig. 2 Estimation errors for the decoupled slow subsystem states

Fig. 4 shows the evolution of the control input and outputs. Evolutions of the states of the original system are represented in Figs. 5 and 6. From the simulation results, a significant improvement in the overall system performance can be observed with the MRSF control compared to single-rate sampling (τ). Moreover, the online computations are reduced compared to single-rate sampling (Δ) with nearly matching performance.

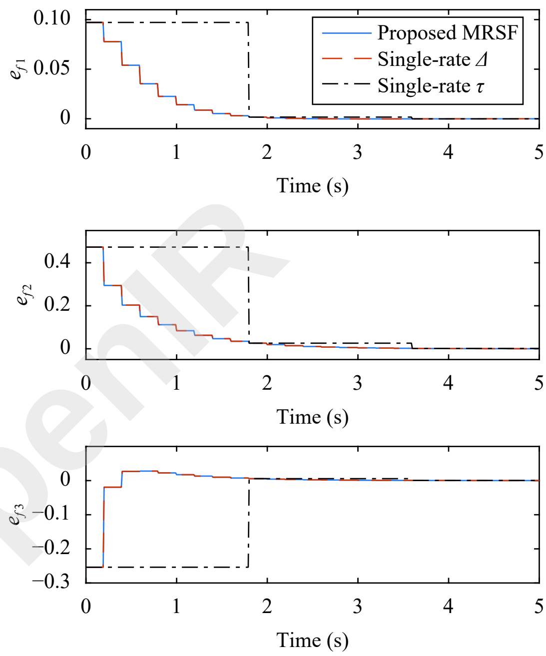

Fig. 3 Estimation errors for the decoupled fast subsystem states

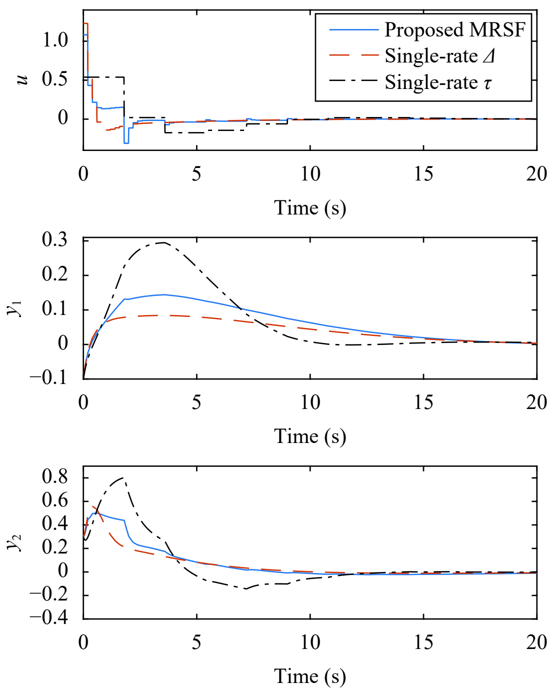

Fig. 4 Evolution of control input and system outputs

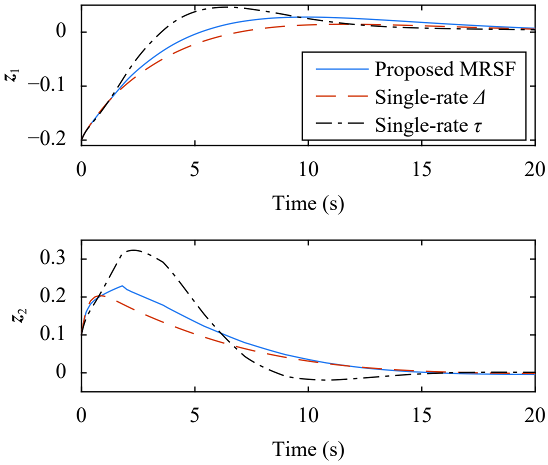

Fig. 5 Evolution of z_1 and z_2 states of the original system

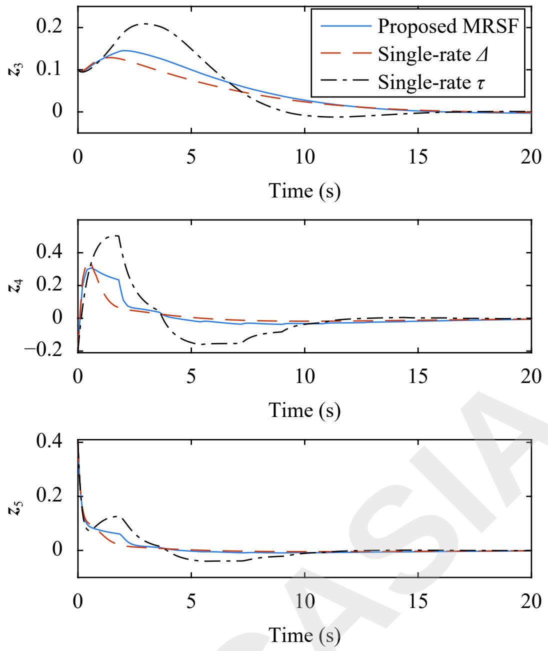

Fig. 6 Evolution of z_3, z_4 and z_5 states of the original system

4 Conclusions

In this paper, a multirate state feedback control scheme is presented for a two-time-scale system using the exact separation of the fast and slow subsystems. The fast subsystem states are sampled at a higher rate than the slow subsystem states. Two steps of subsystem separation and two stages of MRSF control are merged. For control implementation, the decoupled states are computed by a sequential two-stage observer, designed for a continuous two-time-scale system. The proposed control is then applied to an illustrative example and simulations are presented. Simulations are compared with the single-rate sampling and it is observed that the multirate sampling improves system performance. Although the observer is designed in a continuous-time domain in this paper, the multirate state estimation problem may be considered in future.

Acknowledgements

This work was supported by National Natural Science Foundation of China (No. 61750110524) and National Key R&D Program of China (No. 2017YFE0128500).

References

[1] D. P. Glasson. Development and applications of multirate digital control [25 Years Ago]. *IEEE Control Systems Magazine*, vol. 28, no. 5, pp. 13–15, 2008. DOI: 10.1109/MCS.2008.927958.

[2] M. Araki, T. Hagiwara. Pole assignment by multirate sampled-data output feedback. *International Journal of Control*, vol. 44, no. 6, pp. 1661–1673, 1986. DOI: 10.1080/00207178608933692.

[3] A. B. Chammas, C. T. Leondes. Pole assignment by piecewise constant output feedback. *International Journal of Control*, vol. 29, no. 1, pp. 31–38, 1979. DOI: 10.1080/00207177908922677.

[4] T. Hagiwara, M. Araki. Design of a stable state feedback controller based on the multirate sampling of the plant output. *IEEE Transactions on Automatic Control*, vol. 33, no. 9, pp. 812–819, 1988. DOI: 10.1109/9.1309.

[5] Z. Li, S. R. Xue, X. H. Yu, H. J. Gao. Controller optimization for multirate systems based on reinforcement learning. *International Journal of Automation and Computing*, vol. 17, no. 3, pp. 417–427, 2020. DOI: 10.1007/s11633-020-1229-0.

[6] R. K. Munje, B. M. Patre. Fast output sampling controller for three time scale systems. *In Proceedings of Indian Control Conference*, *IEEE*, *Hyderabad*, *India*, pp. 456–460, 2016. DOI: 10.1109/INDIANCC.2016.7441174.

[7] R. K. Munje, B. M. Patre, A. P. Tiwari. Periodic output feedback for spatial control of AHWR: A three-time-scale approach. *IEEE Transactions on Nuclear Science*, vol. 61, no. 4, pp. 2373–2382, 2014. DOI: 10.1109/TNS.2014.2327691.

[8] A. P. Tiwari, G. D. Reddy, B. Bandyopadhyay. Design of periodic output feedback and fast output sampling based controllers for systems with slow and fast modes. *Asian Journal of Control*, vol. 14, no. 1, pp. 271–277, 2012. DOI: 10.1002/asjc.357.

[9] Y. Zhang, D. S. Naidu, C. X. Cai, A. Y. Zou. Singular perturbations and time scales in control theories and applications: An overview 2002–2012. *International Journal of Informaton and Systems Sciences*, vol. 9, no. 1, pp. 1–36, 2014.

[10] A. Tellili, N. Abdelkrim, A. Challouf, M. N. Abdelkrim. Adaptive fault tolerant control of multi-time-scale singularly perturbed systems. *International Journal of Automation and Computing*, vol. 15, no. 1, pp. 736–746, 2018. DOI: 10.1007/s11633-016-0971-9.

[11] R. G. Phillips. Reduced order modelling and control of two-time-scale discrete systems. *International Journal of Control*, vol. 31, no. 4, pp. 765–780, 1980. DOI: 10.1080/00207178008961081.

[12] V. Radisavljevic-Gajic. A simplified two-stage design of linear discrete-time feedback controllers. *Journal of Dynamic Systems*, *Measurement*, *and Control*, vol. 137, no. 1, Article number 014506, 2015. DOI: 10.1115/1.4028153.

[13] V. Radisavljevic-Gajic. Two-stage feedback control design for a class of linear discrete-time systems with slow and

fast modes. *Journal of Dynamic Systems, Measurement, and Control*, vol. 137, no. 8, Article number 084502, 2015. DOI: 10.1115/1.4030088.

[14] B. Litkouhi, H. Khalil. Multirate and composite control of two-time-scale discrete-time systems. *IEEE Transactions on Automatic Control*, vol. 30, no. 7, pp. 645–651, 1985. DOI: 10.1109/TAC.1985.1104024.

[15] H. Kando, T. Iwazumt. Multirate digital control design of an optimal regulator via singular perturbation theory. *International Journal of Control*, vol. 44, no. 6, pp. 1555–1578, 1986. DOI: 10.1080/00207178608933686.

[16] B. Lennarston. Multirate sampled-data control of two-time-scale systems. *IEEE Transactions on Automatic Control*, vol. 34, no. 6, pp. 642–644, 1989. DOI: 10.1109/9.24238.

[17] R. Munje, D. Y. Gu, R. Desai, B. Patre, W. D. Zhang. Observer-based spatial control of advanced heavy water reactor using time-scale decoupling. *IEEE Transactions on Nuclear Science*, vol. 65, no. 11, pp. 2756–2766, 2018. DOI: 10.1109/TNS.2018.2873803.

[18] H. Yoo, Z. Gajic. New designs of reduced-order observer-based controllers for singularly perturbed linear systems. *Mathematical Problems in Engineering*, vol. 2017, Article number 2859548, 2017. DOI: 10.1155/2017/2859548.

[19] H. Yoo, Z. Gajic. New designs of linear observers and observer-based controllers for singularly perturbed linear systems. *IEEE Transactions on Automatic Control*, vol. 63, no. 11, pp. 3904–3911, 2018. DOI: 10.1109/TAC.2018.2814920.

[20] M. Bidani, M. Djemai. A multirate digital control via a discrete-time observer for non-linear singularly perturbed continuous-time systems. *International Journal of Control*, vol. 75, no. 8, pp. 591–613, 2002. DOI: 10.1080/00207170210132978.

[21] H. Kando, H. Ukai, Y. Morita. Design of multirate observers and multirate control systems. *International Journal of Systems Science*, vol. 31, no. 8, pp. 1021–1030, 2000. DOI: 10.1080/002077200412168.

[22] H. Kando, H. Ukai. Design of reduced-order multirate observers and stabilizing multirate controllers via singular perturbation theory. *Optimal Control Applications and Methods*, vol. 19, no. 6, pp. 435–445, 1998.

[23] K. Kumari, B. Bandyopadhyay, K. S. Kim, H. Shim. Output feedback based event-triggered sliding mode control for delta operator systems. *Automatica*, vol. 103, pp. 1–10, 2019. DOI: 10.1016/j.automatica.2019.01.015.

[24] J. A. Isaza, H. A. Botero, H. Alvarez. State estimation using non-uniform and delayed information: A review. *International Journal of Automation and Computing*, *vol.15*, vol. 2, pp. 125–141, 2018. DOI: 10.1007/s11633-017-1106-7.

[25] C. T. Chen, *Linear System Theory and Design*, New York, USA: Oxford University Press, 1999.

[26] P. Kokotovic, H. K. Khalil, J. O'Reilly. *Singular Perturbation Methods in Control*: *Analysis and Design*, Philadelphia, USA: SIAM Publishers, 1999.

[27] D. S. Naidu, A. K. Rao, *Singular Perturbation Analysis of Discrete Control Systems*, Berlin, Germany: Springer-Verlag, 1985.

[28] A. J. Jerri. The Shannon sampling theorem-its various extensions and applications: A tutorial review. *Proceedings of the IEEE*, vol. 65, no. 11, pp. 1565–1596, 1977. DOI: 10.1109/PROC.1977.10771.

[29] F. Ding, L. Qiu, T. W. Chen. Reconstruction of continuous-time systems from their non-uniformly sampled discrete-time systems. *Automatica*, vol. 45, no. 2, pp. 324–332, 2009. DOI: 10.1016/j.automatica.2008.08.007.

[30] G. S. Ladde, S. G. Rajalakshmi. Diagonalization and stability of multi-time-scale singularly perturbed linear systems. *Applied Mathematics and Computation*, vol. 16, no. 2, pp. 115–140, 1985. DOI: 10.1016/0096-3003(85)90003-7.

[31] D. S. Naidu. *Singular Perturbation Methodology in Control Systems*, London, UK: Peter Peregrinus Ltd., 1988. DOI: 10.1049/PBCE034E.

[32] MATLAB. *Simulink Control Design Toolbox User Manual*, Math Works, Version 4.5, [Online], Available: https://in.mathworks.com/help/slcontrol/, 2017.

Ravindra Munje received the B. Eng. degree in electrical from Mumbai University, India in 2005, the M. Eng. degree in control systems from Pune University, India in 2009, and the Ph. D. degree in electrical engineering from Swami Ramanand Teerth Marathwada University, India in 2015. He was a post-doctoral fellow with Shanghai Jiao Tong University, China from June 2017 to May 2019. Currently, he is a professor at Electrical Engineering Department, K. K. Wagh Institute of Engineering Education and Research, India. He has written a book and about 40 refereed papers. He received the Promising Engineer Award in 2016, Outstanding Researcher Award in 2018 and Best Faculty Award in 2019.

His research interests include modeling and control of large-scale systems using sliding mode and multirate output feedback.

E-mail: ravimunje@yahoo.co.in
ORCID iD: 0000-0003-4290-684X

Wei-Dong Zhang received the B. Sc. degree in instrument & measurement, the M. Sc. in instrument & measurement and the Ph. D. degree in industrial automation from Zhejiang University, China in 1990, 1993 and 1996, respectively, and then worked as a postdoctoral fellow at Shanghai Jiao Tong University, China. He joined Shanghai Jiao Tong University as an associate professor in 1998 and has been a full professor since 1999. From 2003 to 2004, he worked at University of Stuttgart, Germany, as an Alexander von Humboldt Fellow. He is a recipient of the National Science Fund for Distinguished Young Scholars of China and Cheung Kong Scholars Program. In 2011, he was appointed Chair Professor at Shanghai Jiao Tong University. He is currently the director of the Engineering Research Center of Marine Automation, Municipal Education Commission. He is the author of more than 300 refereed papers and 1 book and holds 51 patents.

His research interests include control theory and information processing theory and their applications in several fields, including power/chemical processes, USV/ROV and aerocraft.

E-mail: wdzhang@sjtu.edu.cn (Corresponding author)
ORCID iD: 0000-0002-4700-1276